

## Nonreciprocal quantum correlations and dense coding

Muzzamal Iqbal Shaukat <sup>\*</sup>

*School of Natural Sciences, National University of Sciences and Technology, H-12, Islamabad, Pakistan*



(Received 20 January 2022; accepted 31 May 2022; published 15 June 2022)

We compute different quantifiers to analyze the spontaneous generation of entanglement for a unidirectional (nonreciprocal) two-two level system. We illustrate this approach by deriving the Markovian master equation in the Lindblad form. The numerical analysis of the unidirectional master equation enabled to obtain the steady-state concurrence. We explore the quantum dense coding between two spatially separated dipoles taking into account the collective damping effect. Our results reveal the sharp decline and then gradual increase in the dense coding capacity to reach a stable value. This procedure opens the possibility to implement this scheme for further applications in the field of quantum information theory.

DOI: [10.1103/PhysRevA.105.062426](https://doi.org/10.1103/PhysRevA.105.062426)

### I. INTRODUCTION

Quantum information theory is an emerging field to study a great variety of phenomenon such as fundamental quantum science, communication, and computation [1]. An intriguing aspect to understand the information processing is the physical entity qubit, a key feature to exhibit correlations that cannot be accounted classically [2,3]. Last decade, the investigations suggest that entanglement is at the root of the power of quantum computers [4,5]. Over recent years, a great deal of attention has been devoted to measure the quantum correlations using different quantifiers such as concurrence [6–8], negativity [9], and discord [10–13].

Concurrence defined by Woottter [14] is regarded as the most widely spread measure of entanglement. A significant volume of literature has been devoted to the study of entanglement dynamics following concurrence [6–8,15–18]. Furthermore, a recent novel approach of dark-soliton qudits with Bose-Einstein condensates has been introduced to determine the entanglement between long-lived dark soliton qudits [6,15]. Another computable measure of the entanglement is negativity [19], and can be regarded as a quantitative version of Peres' criterion for separability [20]. During last decades, an enormous interested has devoted to another interesting approach of quantum correlations called quantum discord [11,12], where the geometrical measure is defined to be trace distance discord [21]. This approach can also be used to detect quantum phase transitions [22].

From the practical point of view, entanglement is a key resource of two qubit quantum operations such as quantum teleportation [23–25], quantum cryptography [1,26], quantum dense coding [27], and quantum computing [28]. Over recent years, considerable research efforts have been devoted to analyze the quantum dense coding for transmitting classical information by sending an encoded quantum system with the assistance of quantum entanglement [29–32]. The

researches have investigated this aspect for spatially separated two atoms in free space [33], Heisenberg XYZ model [34] and spin model under external magnetic field [21]. Motivated by the recent interest in nonreciprocal platforms, we investigate the nonreciprocal entanglement between two spatially separated two-two level atoms (dipoles) mediated by the plasmonic surface. The scheme is similar to Refs. [35,36] but restricted to unidirectional response. In what follows, we solve the unidirectional master equation numerically to obtain the steady-state concurrence and to explore the application quantum dense coding.

The paper is organized as follows: In Sec. II, we present the theoretical model of spatially separated two-two level atoms (dipoles) placed at distance  $h$  from the plasmonic surface. We also describe the nonreciprocal (unidirectional) master equation to obtain the explicit expressions of the density-matrix evolution. Section III provides different measures to quantify the nonreciprocal entanglement. In the following Sec. IV, we numerically solve the master equation to obtain the steady-state correlation dynamics. Section V contains the realization of quantum dense coding and we present the conclusion in Sec. VI.

### II. THEORETICAL MODEL

We consider a spatially separated two-qubit system interacting with a plasmonic surface placed at distance  $h$  (see Fig. 1). The Hamiltonian corresponding to the total system comprising the two dipole (two level) system and plasmonic surface can be decomposed into three parts

$$\hat{H}_{\text{total}} = \hat{H}_d + \hat{H}_p + \hat{H}_{\text{int}}, \quad (1)$$

where the term  $\hat{H}_d = \hbar\omega_0\hat{\sigma}_z^i/2$  denotes the Hamiltonian of the  $i$ th two-level system with the transition frequency  $\omega_0$  and the inversion operator  $\hat{\sigma}_z = |e\rangle\langle e| - |g\rangle\langle g|$ . The second term  $\hat{H}_p$  represents the Hamiltonian of the plasmonic field given by

$$\hat{H}_p = \sum_{\omega_{\mathbf{nk}} > 0} \frac{\hbar\omega_{\mathbf{nk}}}{2} (\hat{a}_{\mathbf{nk}}^\dagger \hat{a}_{\mathbf{nk}} + \hat{a}_{\mathbf{nk}} \hat{a}_{\mathbf{nk}}^\dagger), \quad (2)$$

<sup>\*</sup>muzzamalshaukat@gmail.com

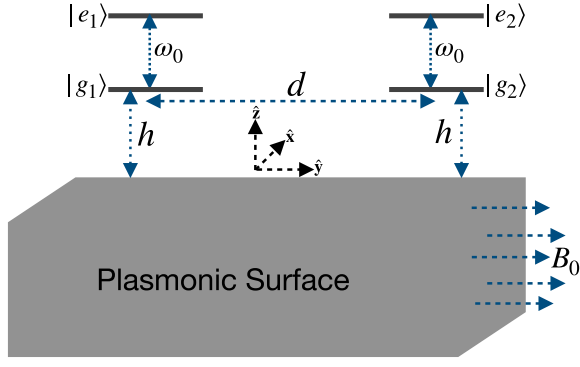


FIG. 1. Theoretical model describes the two dipoles separated by distance  $d$  and placed at distance  $h$  from the plasmonic surface.

where the sum is taken over positive oscillation frequencies  $\omega_{nk}$ , and  $\hat{a}_{nk}^\dagger$  ( $\hat{a}_{nk}$ ) denotes the creation (annihilation) operator of the bosonic field, satisfying the commutation relation  $[\hat{a}_{nk}, \hat{a}_{nk'}^\dagger] = \delta_{k,k'}$ . The term  $\hat{H}_{\text{int}}$  represents the interaction Hamiltonian between the atom and the plasmonic field, denoted by

$$\hat{H}_{\text{int}} = - \sum_j (\tilde{\mathbf{y}}_j^* \hat{\sigma}_+^j + \tilde{\mathbf{y}}_j \hat{\sigma}_-^j) \cdot \hat{\mathbf{F}}(\mathbf{r}_j), \quad (3)$$

$$\mathcal{G}(r_i, r_j) = \frac{1}{8\pi^2 \epsilon_0} \vec{\nabla}_r \left( \int d^2 \mathbf{k}_{\parallel} \tilde{R}(k_x, k_y) \frac{1}{k_{\parallel}} e^{ik_{\parallel}(r_j - r_i)} e^{-k_{\parallel}(z_j + z_i)} \right) \cdot \hat{\mathbf{r}}_0, \quad (6)$$

with

$$\tilde{R}(k_x, k_y) = \frac{\Omega_k}{2} \frac{1}{\omega_k - \omega} + \frac{\Omega_{-k}}{2} \frac{1}{\omega_{-k} + \omega}, \quad (7)$$

and

$$\Omega_{\pm k} = \frac{8\omega_{\pm k} k_{\parallel} \tilde{k}_{\parallel}}{\{2k_{\parallel} \tilde{k}_{\parallel} \pm \partial_{\omega}(\epsilon_r \omega)(\tilde{k}_{\parallel}^2 + k_x^2) \pm \partial_{\omega}(\epsilon_a \omega)k_y^2 + \partial_{\omega}(\epsilon_g \omega)2k_x \tilde{k}_{\parallel}\}}. \quad (8)$$

Here,  $2\omega_k = \omega_c \cos(\theta) + \{2\omega_p^2 + \omega_c^2[1 + \sin^2(\theta)]\}^{1/2}$  with  $\omega_k = (\omega_- \leq \omega_{\theta} \leq \omega_+)$  and  $\omega_{\pm} = \omega_{\theta=0, \pi}$  are the plasmon resonances for propagation along the  $\pm x$  axis, respectively [38]. Here, the function  $\omega_k$  depends only on the wave-vector angle  $\theta$  and does not depend on the magnitude of the wave vector.

We follow the procedure outlined in Ref. [36] to derive the Markovian master equation (see Appendix) for unidirectional system [ $\mathcal{G}(r_1, r_2) = 0$  but  $\mathcal{G}(r_2, r_1) \neq 0$ ] in a way,

$$\begin{aligned} \frac{\partial \rho_d(t)}{\partial t} = & -\frac{i}{\hbar} [H_d, \rho_d(t)] \\ & + \sum_{i=1}^2 \Gamma_{ii} \left[ \sigma_-^i \rho_d(t) \sigma_+^i - \frac{1}{2} \{ \sigma_+^i \sigma_-^i, \rho_d(t) \} \right] \\ & + \lambda_{21} [\sigma_-^2 \rho_d(t) \sigma_+^1 - \rho_d(t) \sigma_+^1 \sigma_-^2] \\ & + \lambda_{21}^* [\sigma_-^1 \rho_d(t) \sigma_+^2 - \rho_d(t) \sigma_+^2 \sigma_-^1], \end{aligned} \quad (9)$$

with

$$\hat{\mathbf{F}}(\mathbf{r}_j) = \sum_{\omega_{nk>0}} \sqrt{\frac{\hbar \omega_{nk}}{2}} \hat{a}_{nk} \mathbf{F}_{nk}(\mathbf{r}_j) + \text{H.c.}, \quad (4)$$

where  $\mathbf{F}_{nk}(\mathbf{r}) = \mathbf{f}_{nk}(z) e^{i\mathbf{k} \cdot \mathbf{r}}$  denotes the electromagnetic modes with the field  $\mathbf{f}_{nk}$  and  $\hat{\mathbf{p}}_d = \tilde{\mathbf{y}}^* \hat{\sigma}_+ + \tilde{\mathbf{y}} \hat{\sigma}_-$  represents the dipole moment with a six-vector  $\tilde{\mathbf{y}} = [\gamma \ 0]^T$ , the dipole moment element  $\gamma$  and the operator  $\hat{\sigma}_+ = |e\rangle\langle g|$  ( $\hat{\sigma}_- = |g\rangle\langle e|$ ). To characterize the nonreciprocal response, the system is biased with a static magnetic field  $B_0$  for which the region  $z > 0$  is filled by vacuum, and that the region  $z < 0$  is filled with a gyrotropic material with permittivity  $\epsilon = \epsilon_0(\epsilon_r \mathbf{I}_t + \epsilon_a \hat{\mathbf{y}} + i\epsilon_g \hat{\mathbf{y}} \times \mathbf{I})$ , where  $\mathbf{I}_t = \mathbf{I} - \hat{\mathbf{y}}\hat{\mathbf{y}}$  and  $\epsilon_g$  determines the strength of the nonreciprocal response. The permittivity elements for the  $+y$  axis biased magnetic field are given by [37,38]

$$\begin{aligned} \epsilon_a &= 1 - \frac{\omega_p^2}{\omega(\omega + i\Gamma)}, \quad \epsilon_t = 1 - \frac{\omega_p^2(1 + i\Gamma/\omega)}{(\omega + i\Gamma)^2 - \omega_c^2}, \\ \epsilon_g &= \frac{1}{\omega} \frac{\omega_c \omega_p^2}{\omega_c^2 - (\omega + i\Gamma)^2}, \end{aligned} \quad (5)$$

where  $\omega_p$  denotes the plasma frequency and  $\omega_c = -qB_0/m > 0$  represents the cyclotron frequency with the electron charge  $q = -e$  and the effective electron mass  $m$ . Therefore, the communication between two qubits (dipoles), restricted to nonreciprocal system (unidirectional), leads to

where  $\lambda_{21} = (\Gamma_{21} + 2ig_{21})/2$ . Here  $\Gamma_{ii}$  represents the spontaneous emission rate of  $i$ th dipole and

$$\begin{aligned} \Gamma_{21} &= \frac{2}{\hbar} \text{Im}\{\tilde{\mathbf{y}}_i^* \cdot \mathcal{G}(\mathbf{r}_2, \mathbf{r}_1; \omega_0) \cdot \tilde{\mathbf{y}}_j\}, \\ g_{21} &= \frac{1}{\hbar} \text{Re}\{\tilde{\mathbf{y}}_i^* \cdot \mathcal{G}(\mathbf{r}_2, \mathbf{r}_1; \omega_0) \cdot \tilde{\mathbf{y}}_j\}, \end{aligned} \quad (10)$$

denotes the collective damping and dipole-dipole interaction, respectively. Furthermore, both two level systems are assumed to be identical and taking  $\Gamma_{11} = \Gamma_{22}$ . It is pertinent to mention here that the derived master equations satisfy the completely positive trace preserving conditions in accordance with the procedure outlined in Refs. [39,40].

Figure 2 shows the collective damping [Fig. 2(a)] and dipole-dipole interaction [Fig. 2(b)] as a function of dipole-dipole separation  $d$ . It is shown that, for large separations, i.e.,  $d \gg h$ , both parameters are very small ( $\Gamma_{12} \approx g_{12} \approx 0$ ). When the atom transition frequency is tuned to the SPP

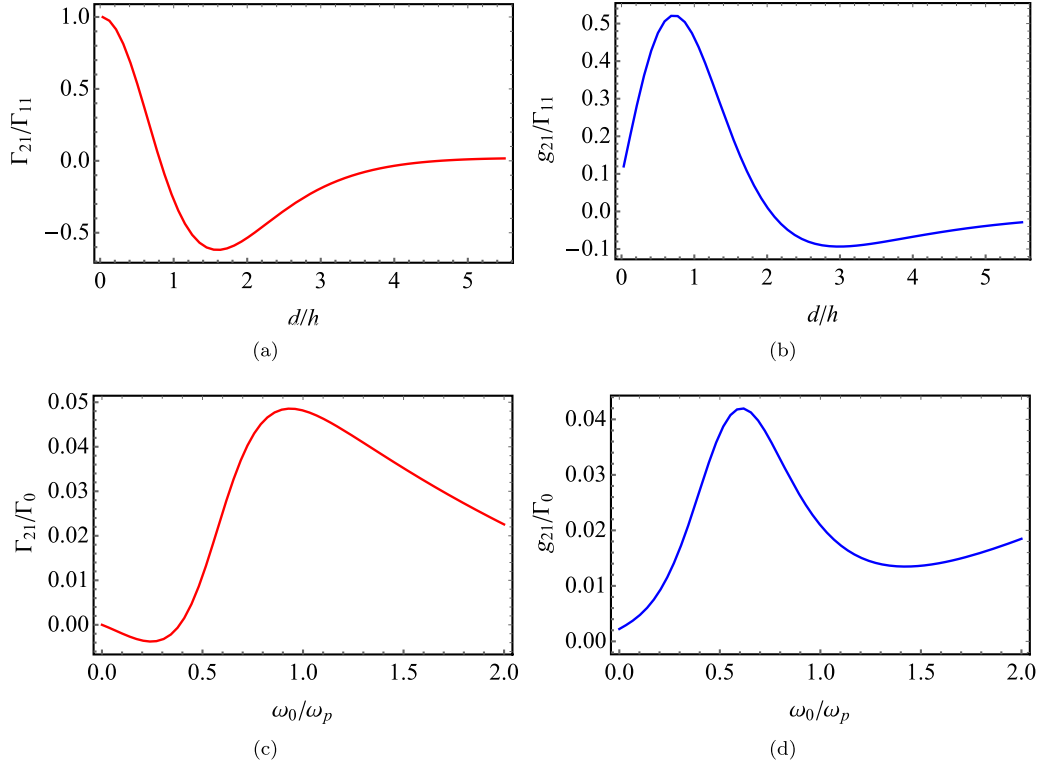


FIG. 2. Panels (a) and (b) explore the collective damping  $\Gamma_{21}$  and qubit-qubit interaction  $g_{21}$ , respectively for nonreciprocal system as a function of the dipole-dipole separation  $d$ , where  $\omega_c = 0.4\omega_p$ ,  $\omega_0 = 0.1\omega_p$ ,  $\Gamma = 0.1\omega_p$ , and  $2\omega_k = -\omega_c + (\omega_c^2 + 2\omega_p^2)^{1/2}$ . Panels (c) and (d) depict the variation of  $\Gamma_{21}$  and  $g_{21}$  as a function of transition frequency  $\omega_0$ , where  $\Gamma_0 = |\tilde{\gamma}^2|/4\pi\epsilon_0\hbar d^3$  and the remaining parameters are the same as those for panels (a) and (b).

resonance ( $\omega_0 \simeq \omega_{sp}$ ), the function  $\Gamma_{12}$  is maximum and  $g_{12}$  is negligibly small.

### III. MEASURES OF QUANTUM CORRELATION

The basic peculiarity between classical and quantum dynamics is the entanglement and how to quantify it is the central topic within quantum information theory. To compute the entanglement dynamics, we are considering the Dicke bases ( $|e\rangle = |e_1, e_2\rangle$ ,  $|g\rangle = |g_1, g_2\rangle$ ), and  $|\pm\rangle = (|e_1, g_2 \pm g_1, e_2\rangle/\sqrt{2})$  [41] for which the density-matrix elements of the nonreciprocal master equation (9) for the initial state  $(|+\rangle + |-\rangle)/\sqrt{2}$  are given by

$$\begin{aligned}\rho_{\pm\pm}(t) &= \frac{1}{2}e^{-\Gamma_{11}t}(\mp 1 + \lambda_{21}t)(\mp 1 + \lambda_{21}^*t), \\ \rho_{\pm\mp}(t) &= \frac{1}{2}e^{-\Gamma_{11}t}(\pm 1 + \lambda_{21}t)(\mp 1 + \lambda_{21}^*t), \\ \rho_{gg}(t) &= e^{-\Gamma_{11}t}(-1 + e^{\Gamma_{11}t} - \lambda_{21}\lambda_{21}^*t^2),\end{aligned}\quad (11)$$

where all remaining elements are zero. To compute the degree of correlations, we present three different entanglement measures.

#### A. Concurrence

A most widely spread measure defined by Woottter [14] is the concurrence,

$$C_{nr}(t) = 2\sqrt{\lambda_{21}\lambda_{21}^*}te^{-\Gamma_{11}t}.\quad (12)$$

By defining the parameter  $\lambda_{21} = \gamma_R e^{ikd}$  in close analogy to Ref. [36], we can modify Eq. (12) to describe the chiral route concurrence  $C_c(t) = 2\gamma_R t e^{-\Gamma_{11}t}$ , which determines the independence of concurrence from the qubit separation  $d$ . The transient evolution of concurrence for an initial state  $(|+\rangle + |-\rangle)/\sqrt{2}$  is shown in Fig. 3. The concurrence exhibits the fast increase followed by a slow decay and reaches to subradiant state  $|-\rangle$ .

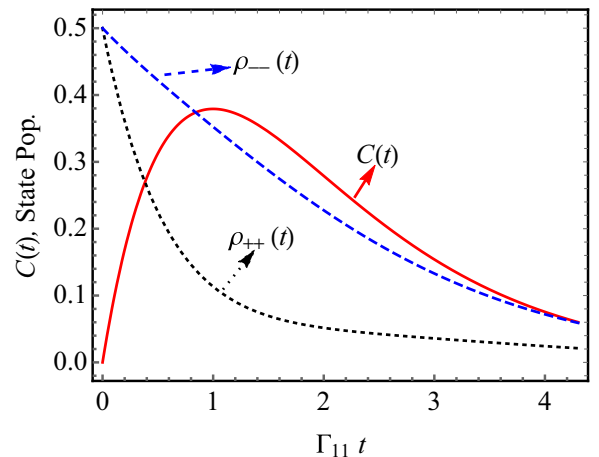


FIG. 3. Time evolution of transient concurrence  $C(t)$ , the population of symmetric state  $|+\rangle$  and antisymmetric state  $|-\rangle$  between two dipoles, polarized along horizontal axis ( $\tilde{\gamma} = \gamma\hat{x}$ ) and separated by distance  $d \simeq h/2$ . The other parameters are same as in Fig. 2.

Controlling light-matter interaction is the basis for diverse applications ranging from light technology to quantum-information processing. The directional exchange of mediating particle between emitters offers interesting novel perspective for many-body quantum dynamics. Chiral quantum optics is a new paradigm to investigate the light matter interaction, where the light propagates differently in the forward or backward direction and can be unidirectional (non-reciprocal) in the most extreme cases [42]. The researchers have investigated this theory in the context of emitters chirally coupled to waveguides, theoretically and experimentally [43,44]. For example, consider the spontaneous emission of an ensemble of two-level emitters. Due to the collective character of the bath, the emission differs strongly from that of independent emitters [16], an effect referred to as subradiance and superradiance [41]. One of the main differences between the concurrence in the reciprocal [6–8] and nonreciprocal [16] case is the presence of the sinusoidal term (due to qubit-qubit interaction  $g_{21}$ ) in the reciprocal medium, causes oscillations in the transient concurrence (recycled mediating particle with a period corresponds to the round trip time of the coupled qubits), which does not occur in nonreciprocal case. The other advantage of the unidirectional case is that the qubit positioning is unimportant [45], and the qubits can be anywhere in the coherent or dissipative regimes, which is a practical advantage of the unidirectional systems.

### B. Logarithmic negativity

Another computable measure of entanglement is the logarithmic entropy defined by [9]

$$N_{nr}(t) = \text{Max}\{0, \log_2[1 - \rho_{gg} + \sqrt{\rho_{gg}^2 + |\alpha|^2}]\}, \quad (13)$$

with  $|\alpha|^2 = (\rho_{++} - \rho_{--})^2 - (\rho_{+-} - \rho_{-+})^2$ . An analytical expression of the logarithmic negativity can be determined by substituting Eq. (11) into Eq. (13).

### C. Trace distance discord

Third measure to analyze the entanglement between two-level system is the trace distance discord given by [21]

$$D_{nr}(t) = \sqrt{\frac{v_1^2 \lambda_{\max} - v_2^2 \lambda_{\min}}{v_1^2 - v_2^2 + \lambda_{\max} - \lambda_{\min}}}, \quad (14)$$

where  $v_1 = (\alpha + 2|\rho_{eg}|)$ ,  $v_2 = (\alpha - 2|\rho_{eg}|)$ ,  $\lambda_{\min} = \min\{v_1^2, v_2^2\}$ , and  $\lambda_{\max} = \max\{v_3^2, v_2^2 + \Lambda^2\}$ , with  $v_3 = 1 - 2(\rho_{++} + \rho_{--})$  and  $\Lambda = 2(\rho_{gg} + \rho_{++}) - 1$ . Using density-matrix elements of Eq. (11) and simplifying Eq. (14), we obtained the analytical expression of the trace distance discord, i.e.,

$$D_{nr}(t) = 2\sqrt{\lambda_{21}\lambda_{21}^*} t e^{-\Gamma_{11}t} = C_{nr}(t). \quad (15)$$

Figure 4 depicts the time evolution of the entanglement quantifiers  $[C_{nr}(t), N_{nr}(t), D_{nr}(t)]$  for an initial superposition of super-radiant  $|+\rangle$  and subradiant  $|-\rangle$  states. It is observed that the concurrence  $C_{nr}(t)$  and the trace distance discord  $D_{nr}(t)$  have the same behavior in accordance with Eq. (15). However, the entropy  $N_{nr}(t)$  takes smaller values and decays faster than the concurrence.

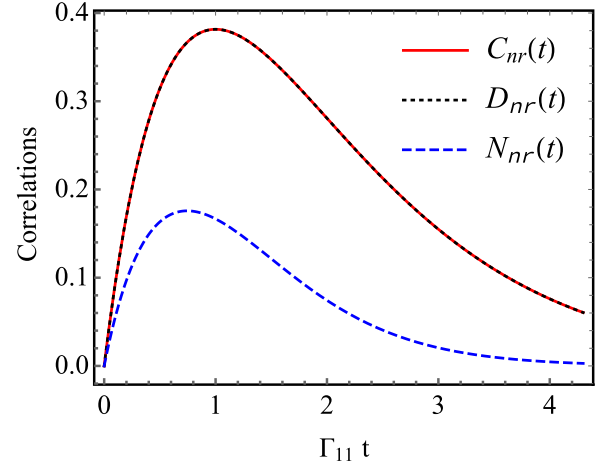


FIG. 4. Time evolution of quantum correlations with concurrence (red), trace distance discord (dotted black) and the logarithmic negativity (dashed blue).

## IV. STEADY-STATE CONCURRENCE

In what follows Sec. II, we now turn to analyze the steady-state entanglement by using the Wootters' criteria [14], described by the Hamiltonian

$$H_d = \hbar \sum_{j=1}^2 \Omega_j [\sigma_+^{(j)} + \sigma_-^{(j)}] \quad (16)$$

for both dipoles externally pumped by a laser with Rabi frequency  $\Omega_j$  ( $j = 1, 2$ ), respectively. We solve the master equation (9) including the driven Hamiltonian (16) numerically to extract the steady-state concurrence. Figure 5 demonstrates that unequal pumping leads to larger steady-state concurrence, achieved after a long time ( $\Gamma_{11}t = 8$ ).

## V. QUANTUM DENSE CODING

In this section, we realize the dense coding in detail between two spatially separated two-level systems, which describes the transmission of two classical bits of information by sending one qubit with the assistance of

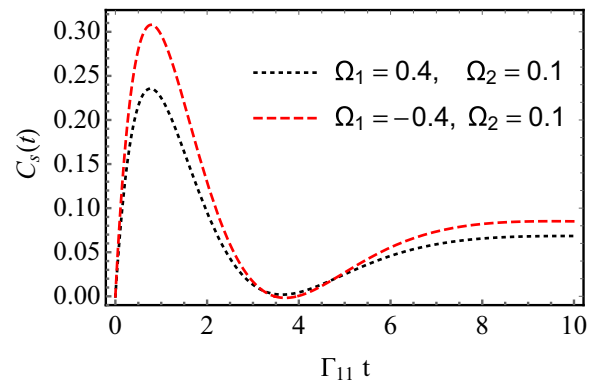


FIG. 5. Steady-state concurrence with the pumping intensities of two qubits at distance  $d \simeq h/3$  (dashed red) and  $d \simeq 3h/2$  (dotted black). The other parameters are the same as in Fig. 2.

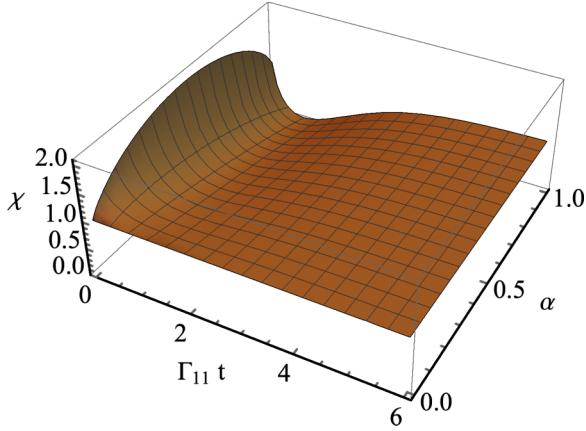


FIG. 6. Transient evolution of superdense coding  $\chi$  with the parameter  $\alpha$  at  $d = h/2$ .

entanglement [27]. This work has experienced an extraordinary renaissance, theoretically [46–48] and experimentally [45,49]. To obtain the information capacity, the quantum system sent through an arbitrary quantum channel must be encoded by the unitary operators with the shared entangled state between the sender (Alice) and the receiver (Bob). The set of  $U_{00}|m\rangle \rightarrow |m\rangle$ ,  $U_{01}|m\rangle \rightarrow |m+1(\text{mod}2)\rangle$ ,  $U_{10}|m\rangle \rightarrow e^{i\pi m}|m\rangle$ , and  $U_{11}|m\rangle \rightarrow e^{i\pi m}|m+1(\text{mod}2)\rangle$  (with  $|m\rangle = |0\rangle, |1\rangle$ ) denotes the single qubit computational basis) are performed to obtain the evolution of dense coding capacity. Here

$$\begin{aligned} U_{00} &= \begin{pmatrix} 1 & 0 \\ 0 & 1 \end{pmatrix}, & U_{10} &= \begin{pmatrix} 1 & 0 \\ 0 & -1 \end{pmatrix}, \\ U_{01} &= \begin{pmatrix} 0 & 1 \\ 1 & 0 \end{pmatrix}, & U_{11} &= \begin{pmatrix} 0 & 1 \\ -1 & 0 \end{pmatrix}. \end{aligned} \quad (17)$$

A dense coding capacity can be written as

$$\chi = S(\bar{\rho}^*) - S(\rho), \quad (18)$$

where  $S(\rho) = -\text{Tr}(\rho \log_2 \rho)$  with

$$\bar{\rho}^* = \frac{1}{4} \sum_{i=0}^3 (U_i \otimes I_d) \rho (I_d \otimes U_i^\dagger), \quad (19)$$

$\chi > \log_2[2] = 1$ . To characterize the optimal dense coding capacity, the dipoles are chosen to be initially prepared in a maximally entangled state of the form  $|\Psi\rangle = \sqrt{\alpha}|e\rangle + \sqrt{1-\alpha}|g\rangle$  for which the density-matrix elements are given by

$$\begin{aligned} \rho_{ee}(t) &= \alpha e^{-2\Gamma_{11}t}, & \rho_{eg}(t) &= \sqrt{\alpha(1-\alpha)} e^{-\Gamma_{11}t}, \\ \rho_{\pm\pm}(t) &= \frac{1}{2\Gamma_{11}^2} e^{-2\Gamma_{11}t} \left\{ -2\alpha[2\lambda_{21}\lambda_{21}^* + \Gamma_{11}(\Gamma_{11} \pm \Gamma_{21})] \right. \\ &\quad \left. + \alpha e^{\Gamma_{11}t} [\{\lambda_{21}\lambda_{21}^*(-2 + \Gamma_{11}t) \mp \Gamma_{11}\Gamma_{21}\}] \right. \\ &\quad \left. \times (-2 + \Gamma_{11}t) + 2\Gamma_{11}^2 \right\}, \\ \rho_{\pm\mp}(t) &= \frac{1}{2\Gamma_{11}^2} e^{-2\Gamma_{11}t} \{4\alpha(\lambda_{21}\lambda_{21}^* \pm ig_{21}\Gamma_{11}) - \alpha e^{\Gamma_{11}t} \\ &\quad \times (-2 + \Gamma_{11}t)[\lambda_{21}\lambda_{21}^*(-2 + \Gamma_{11}t) \mp 2ig_{21}\Gamma_{11}]\}, \end{aligned} \quad (20)$$

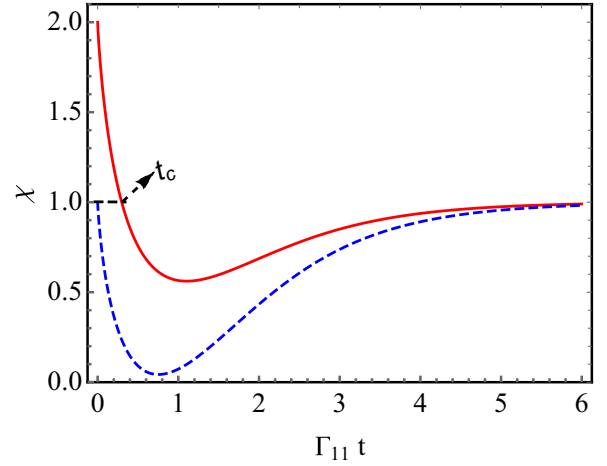


FIG. 7. Transient evolution of superdense coding  $\chi$  for maximally entangled state  $(|e\rangle + |g\rangle)/\sqrt{2}$  (solid red) and pure state  $|e\rangle$  (dashed blue), where  $\alpha = 1/2$ .

with  $\rho_{gg}(t) = 1 - \rho_{ee}(t) - \rho_{++}(t) - \rho_{--}(t)$  and  $\rho_{ij}(t) = \rho_{ji}^*(t)$ . For the pure state  $|e\rangle$  ( $\alpha = 1$ ), the density-matrix elements  $\rho_{eg}(t) = \rho_{ge}(t)$  of Eq. (20) are zero and the remaining elements are reduced by a factor of two. Figure 6 depicts the transient evolution of optimal dense coding with the parameter  $\alpha$ . The optimal dense coding is not permissible for  $\alpha = 0$  because  $|\Psi\rangle = |g\rangle$ . Note that the increase in parameter  $\alpha$  generates the maximally entangled state ( $\alpha = 1/2$ ) for which the dense coding capacity  $\chi$  will always have the maximum optimal value of 2 at  $\Gamma_{11}t = 0$ . It is also depicted that the optimal dense coding exists for  $t < t_c$ , where  $\chi > 1$  (see Fig. 7). Furthermore, the region  $t > t_c$  ( $\chi < 1$ ) determines that the optimal coding is not permissible for this quantum channel.

## VI. CONCLUSION

To conclude, we have explored the entanglement between two-two level systems for nonreciprocal plasmonics. In what follows, we derive the Markovian master equation to extract the collective damping and dipole-dipole interaction functions which modify the entanglement dynamics significantly. Different quantifiers are used to measure the entanglement and, to obtain the analytical expression of concurrence and trace distance discord. The numerical analysis of the unidirectional master equation enabled to obtain the steady-state concurrence. This creates the opportunity to realize the quantum dense coding scheme between two-two level systems. The obtained results confirm the sharp decline and then gradual increase in the dense coding capacity to reach a stable value. This work paved the way to explore a possible important applications in quantum information theory.

## APPENDIX: DERIVATION OF BORN-MARKOV MASTER EQUATION

The Liouville–von Neumann equation by writing the global density matrix  $\rho_{QP}$  is found to be

$$\frac{d\rho_{QP}}{dt} = -\frac{i}{\hbar} [H_0 + H_{\text{int}}, \rho_{QP}], \quad (A1)$$

where  $H_0 = H_d + H_p$ . It is convenient to write Eq. (A1) in the interaction picture of  $H_0$ , for which we define

$$H_{\text{int}}(t) = e^{\frac{i}{\hbar}H_0 t} H_{\text{int}} e^{-\frac{i}{\hbar}H_0 t}, \quad (\text{A2})$$

and

$$\rho(t) = e^{-\frac{i}{\hbar}H_0 t} \rho_Q e^{\frac{i}{\hbar}H_0 t}. \quad (\text{A3})$$

With the new definition of the Hamiltonian and density operator, we can decompose Eq. (A1) as

$$\rho(t) = \rho(t_0) - \frac{i}{\hbar} \int_{t_0}^t [H(\tau), \rho(\tau)] d\tau. \quad (\text{A4})$$

Using Eq. (A4) in Eq. (A1), we get

$$\begin{aligned} \partial_t \rho = & -\frac{i}{\hbar} [H_{\text{int}}(t), \rho(t_0)] \\ & + \frac{1}{\hbar^2} \left[ H_{\text{int}}(t), \int_{t_0}^t [H_{\text{int}}(\tau), \rho(\tau)] d\tau \right]. \end{aligned} \quad (\text{A5})$$

With the Markov approximation and letting  $t_0 \rightarrow -\infty$ , it is possible to write

$$\begin{aligned} \partial_t \rho = & \frac{i}{\hbar} [\rho(t_0), H_{\text{int}}(t)] \\ & - \frac{1}{\hbar^2} \int_0^\infty [[\rho(t), H_{\text{int}}(t - \tau)], H_{\text{int}}(t)] d\tau. \end{aligned} \quad (\text{A6})$$

Let assume that the density matrix is of the form  $\rho = \sum_n p_n |n(t), E_0\rangle \langle n(t), E_0|$  at all times, so that the degrees of freedom of the environment are to a first approximation unaffected by the dynamics of the atom (Born approximation). Thus, defining  $\rho_s = \sum_E 1_s \otimes \langle E | \rho_I 1_s \otimes | E \rangle = \text{tr}_E \rho_I(t)$ , it follows that  $\text{tr}_E [[\rho(t_0), H_{\text{int}}(t)]] = 0$ ,

$$\partial_t \rho_s = -\frac{1}{\hbar^2} \int_0^\infty \text{tr}_E [[\rho(t), H_{\text{int}}(t - \tau)], H_{\text{int}}(t)] d\tau, \quad (\text{A7})$$

where

$$\begin{aligned} H_{\text{int}} = & -\sum_j (\tilde{\gamma}_j^* \sigma_+^j e^{i\omega_0 j t} + \tilde{\gamma}_j \sigma_-^j e^{-i\omega_0 j t}) \cdot \hat{F}(r_j, t) \\ \hat{F}(r, t) = & \sum_{\omega_{nk} > 0} \sqrt{\frac{\hbar \omega_{nk}}{2}} [\hat{a}_{nk} e^{-i\omega_{nk} t} F_{nk}(r)] + \text{H.c.} \end{aligned} \quad (\text{A8})$$

Equation (A7) is the Born-Markov master equation. To proceed, we assume that the environment is in the ground state for which we define the parameter

$$A_\omega^{ij} = \frac{1}{\hbar^2} \sum_{\omega_{nk} > 0} \varepsilon_{0, \omega_{nk}} \frac{1}{i(\omega_{nk} - \omega - i0^+)} F_{nk}^*(r_i) F_{nk}^*(r_j), \quad (\text{A9})$$

where  $\varepsilon_{0, \omega_{nk}} = \hbar |\omega_{nk}|/2$ . Hereafter, we introduce a frequency domain Green's function  $\mathcal{G} = \mathcal{G}^+ + \mathcal{G}^- + M_\infty^{-1} \delta(r - r_0)/i\omega$ , where  $\mathcal{G}^\pm = -i\omega \bar{\mathcal{G}}^\pm$  denotes the positive and negative frequency parts of the Green's function,

$$\begin{aligned} \mathcal{G}^+ = & \sum_{\omega_{nk} > 0} \frac{\omega_{nk}}{2} \frac{1}{\omega_{nk} - \omega} F_{nk}(r_i) \otimes F_{nk}^*(r_j), \\ \mathcal{G}^- = & \sum_{\omega_{nk} > 0} \frac{\omega_{nk}}{2} \frac{1}{\omega_{nk} + \omega} F_{nk}^*(r_i) \otimes F_{nk}(r_j), \end{aligned} \quad (\text{A10})$$

corresponds to the poles on the positive and negative real frequency axes, respectively. Therefore, Eq. (A9) can be written as

$$A_\omega^{ij} = \frac{1}{i\hbar} (-i\omega \bar{\mathcal{G}}^+)(r_i, r_j; \omega - i0^+). \quad (\text{A11})$$

Using  $([-i\omega \bar{\mathcal{G}}^+(r_i, r_j, \omega)]|_{-\omega} = [-i\omega \bar{\mathcal{G}}^-(r_i, r_j, \omega)]^*|_{\omega^*}$ , we introduce

$$\begin{aligned} g_{ij}^\pm = & \frac{1}{\hbar} \text{Re}\{\tilde{\gamma}_i^* \cdot \mathcal{G}^\pm(r_i, r_j; \omega_0) \cdot \tilde{\gamma}_j\}, \\ \Gamma_{ij}^\pm = & \frac{2}{\hbar} \text{Im}\{\tilde{\gamma}_i^* \cdot \mathcal{G}^\pm(r_i, r_j; \omega_0) \cdot \tilde{\gamma}_j\}. \end{aligned} \quad (\text{A12})$$

Therefore, Eq. (A7) can be written as

$$\begin{aligned} \partial_t \rho_s(t) = & \sum_{i,j} \left( \frac{\Gamma_{ij}^+}{2} + i g_{ij}^+ \right) [\sigma_-^i \rho_s(t) \sigma_+^j - \rho_s(t) \sigma_+^j \sigma_-^i] \\ & + \sum_{i,j} \left( \frac{\Gamma_{ij}^+}{2} - i g_{ij}^+ \right) [\sigma_-^j \rho_s(t) \sigma_+^i - \sigma_+^i \sigma_-^j \rho_s(t)] \\ & + \sum_{i,j} \left( \frac{\Gamma_{ij}^-}{2} + i g_{ij}^- \right) [\sigma_-^i \sigma_+^j \rho_s(t) - \sigma_+^j \rho_s(t) \sigma_-^i] \\ & + \sum_{i,j} \left( \frac{\Gamma_{ij}^-}{2} - i g_{ij}^- \right) [\rho_s(t) \sigma_-^j \sigma_+^i - \sigma_+^i \rho_s(t) \sigma_-^j]. \end{aligned} \quad (\text{A13})$$

By employing the series expansion, it is easy to verify for the nonresonant part (−) of the Green's function that  $\Gamma_{ii}^- = 0$ ,  $\Gamma_{ij}^- = -\Gamma_{ji}^-$ , and  $g_{ij}^- = g_{ji}^-$ . Using the relations  $\hat{\sigma}_z = 2\hat{\sigma}_+ \hat{\sigma}_- - 1$ ,  $\hat{\sigma}_- \hat{\sigma}_+ = 1 - \hat{\sigma}_+ \hat{\sigma}_-$  and again transforming Eq. (A13) to the Schrödinger picture, we obtain

$$\begin{aligned} \partial_t \rho_s(t) = & -\frac{i}{2} \sum_i (\omega_0 + g_{ii}^- - g_{ii}^+) [\sigma_z^i, \rho_s(t)] \\ & - \sum_{i,j} \frac{\Gamma_{ij}}{2} [\sigma_+^i \sigma_-^j \rho_s(t) + \rho_s(t) \sigma_+^j \sigma_-^i - \sigma_-^j \rho_s(t) \sigma_+^i \\ & - \sigma_-^i \rho_s(t) \sigma_+^j] + \sum_{i \neq j} i g_{ij} [\sigma_+^i \sigma_-^j \rho_s(t) \\ & - \sigma_-^j \rho_s(t) \sigma_+^i] + \text{H.c.}, \end{aligned} \quad (\text{A14})$$

where

$$\begin{aligned} \Gamma_{ij} = & \frac{2}{\hbar} \text{Im}\{\tilde{\gamma}_i^* \cdot \mathcal{G}(r_i, r_j, \omega_0) \cdot \tilde{\gamma}_j\}, \\ g_{ij} = & \frac{1}{\hbar} \text{Re}\{\tilde{\gamma}_i^* \cdot \mathcal{G}(r_i, r_j, \omega_0) \cdot \tilde{\gamma}_j\}. \end{aligned} \quad (\text{A15})$$

Equation (A14) determines the Markovian master equation, valid for both reciprocal and nonreciprocal systems [putting  $\mathcal{G}(r_1, r_2) = 0$ ] and used to obtain elegant description of physics involved in the dynamics of interacting atoms. Equation (A14) is consistent with the results of Refs. [8,16].

- [1] M. A. Nielsen and I. L. Chuang, *Quantum Computation and Quantum Information* (Cambridge University Press, Cambridge, 2000).
- [2] I. Buluta, S. Ashhab, and F. Nori, *Rep. Prog. Phys.* **74**, 104401 (2011).
- [3] M. I. Shaukat, E. V. Castro, and H. Terças, *Phys. Rev. A* **95**, 053618 (2017).
- [4] G. Vidal, *Phys. Rev. Lett.* **91**, 147902 (2003); **93**, 040502 (2004).
- [5] Z. Ficek and R. Tanas, *Phys. Rev. A* **74**, 024304 (2006).
- [6] M. I. Shaukat, E. V. Castro, and H. Terças, *Phys. Rev. A* **99**, 042326 (2019).
- [7] A. Gonzalez-Tudela, D. Martin-Cano, E. Moreno, L. Martin-Moreno, C. Tejedor, and F. J. Garcia-Vidal, *Phys. Rev. Lett.* **106**, 020501 (2011).
- [8] Z. Ficek and R. Tanas, *Phys. Rep.* **372**, 369 (2002).
- [9] S. Bougouffa, *Opt. Commun.* **283**, 2989 (2010).
- [10] A. Slaoui, M. I. Shaukat, M. Daoud, and R. Ahl Laamara, *Eur. Phys. J. Plus* **133**, 413 (2018).
- [11] H. Ollivier and W. H. Zurek, *Phys. Rev. Lett.* **88**, 017901 (2001); L. Henderson and V. Vedral, *J. Phys. A: Math. Gen.* **34**, 6899 (2001).
- [12] K. Modi, A. Brodutch, H. Cable, T. Paterek, and V. Vedral, *Rev. Mod. Phys.* **84**, 1655 (2012).
- [13] M. I. Shaukat, A. Slaoui, H. Terças and M. Daoud, *Eur. Phys. J. Plus* **135**, 357 (2020).
- [14] W. K. Wootters, *Phys. Rev. Lett.* **80**, 2245 (1998).
- [15] M. I. Shaukat, E. V. Castro, and H. Terças, *Phys. Rev. A* **98**, 022319 (2018).
- [16] S. A. H. Gangaraj, G. W. Hanson, M. Antezza, *Phys. Rev. A* **95**, 063807 (2017).
- [17] M. I. Shaukat, A. Shaheen, and A. H. Toor, *J. Mod. Opt.* **60**, 1937 (2013).
- [18] Z. Ficek, R. Tanas, *Phys. Rev. A* **77**, 054301 (2008).
- [19] G. Vidal and R. F. Werner, *Phys. Rev. A* **65**, 032314 (2002).
- [20] A. Peres, *Phys. Rev. Lett.* **77**, 1413 (1996).
- [21] S. Ahadpour and F. Mirmasoudi, *Rev. Mex. Fís.* **66**, 356 (2020).
- [22] W. W. Cheng, X. Y. Wang, Y. B. Sheng, L. Y. Gong, S. M. Zhao, and J. M. Liu, *Sci. Rep.* **7**, 42360 (2017); R. j. Zhang, S. Xu, J. D. Shi, W. Ma, and L. Ye, *Quant. Info. Proc.* **14**, 4077 (2015).
- [23] C. H. Bennett, G. Brassard, C. Crepeau, R. Jozsa, A. Peres, and W. K. Wootters, *Phys. Rev. Lett.* **70**, 1895 (1993).
- [24] D. Boschi, S. Branca, F. De Martini, L. Hardy, and S. Popescu, *Phys. Rev. Lett.* **80**1121 (1998).
- [25] S. Haroche and J. M. Raimond, *Exploring the Quantum* (Oxford University Press, 2006).
- [26] A. K. Ekert, *Phys. Rev. Lett.* **67**, 661 (1991).
- [27] C. H. Bennett and S. J. Wiesner, *Phys. Rev. Lett.* **69**, 2881 (1992).
- [28] H. J. Briegel and R. Raussendorf, *Phys. Rev. Lett.* **86**, 910 (2001); R. Raussendorf and H. J. Briegel, *ibid.* **86**, 5188 (2001).
- [29] M. Kiffner, J. Evers, and C. H. Keitel, *Phys. Rev. A* **75**, 032313 (2007).
- [30] M. Macovei, Z. Ficek, and C. H. Keitel, *Phys. Rev. A* **73**, 063821 (2006).
- [31] J. Evers, M. Kiffner, M. Macovei, and C. H. Keitel, *Phys. Rev. A* **73**, 023804 (2006).
- [32] G. S. Agarwal and A. K. Patnaik, *Phys. Rev. A* **63**, 043805 (2001).
- [33] Y. Q. Li, X. Li, X. F. Jia, and G. H. Yang, *Int. J. Theor. Phys.* **59**, 3378 (2020).
- [34] H. Y. Xu and G. H. Yang, *Int. J. Theor. Phys.* **56**, 2803 (2017).
- [35] S. Lannebere, M. G. Silveirinha, *J. Opt. (Bristol, U. K.)* **19**, 014004 (2017).
- [36] M. I. Shaukat and M. G. Silveirinha (unpublished).
- [37] J. A. Bittencourt, *Fundamentals of Plasma Physics*, 3rd ed. (Springer-Verlag, New York, 2010).
- [38] M. G. Silveirinha, S. A. Gangaraj, G. W. Hanson, and M. Antezza, *Phys. Rev. A* **97**, 022509 (2018).
- [39] D. Manzano, *AIP Adv.* **10**, 025106 (2020).
- [40] D. A. Lidar, Z. Bihary, and K. B. Whaley, *Chem. Phys.* **268**, 35 (2001).
- [41] R. H. Dicke, *Phys. Rev.* **93**, 99 (1954).
- [42] P. Lodahl, S. Mahmoodian, S. Stobbe, A. Rauschenbeutel, P. Schneeweiss, J. Volz, H. Pichler, and P. Zoller, *Nature (London)* **541**, 473 (2017).
- [43] T. Ramos, H. Pichler, A. J. Daley, and P. Zoller, *Phys. Rev. Lett.* **113**, 237203 (2014).
- [44] J. Petersen, J. Volz, and A. Rauschenbeutel, *Science* **346**, 67 (2014).
- [45] C. Gonzalez-Ballester, A. Gonzalez-Tudela, F. J. Garcia-Vidal, and E. Moreno, *Phys. Rev. B* **92**, 155304 (2015).
- [46] A. Barenco and A. Ekert, *J. Mod. Opt.* **42**, 1253 (1995).
- [47] S. Bose, M. B. Plenio, and V. Vedral, *J. Mod. Opt.* **47**, 291 (2000).
- [48] X. Zhao, Y. Q. Li, L. Y. Cheng, and G. H. Yang, *Int. J. Theor. Phys.* **58**, 493 (2019).
- [49] K. Mattle, H. Weinfurter, P. G. Kwiat, and A. Zeilinger, *Phys. Rev. Lett.* **76**, 4656 (1996).